Solid-State 19 F NMR Spectroscopy Reveals That Trp 41 Participates in the Gating Mechanism of the M2 Proton Channel of Influenza A Virus

ARTICLE *in* JOURNAL OF THE AMERICAN CHEMICAL SOCIETY · FEBRUARY 2008

Impact Factor: 12.11 · DOI: 10.1021/ja0754305 · Source: PubMed

J|A|C|S
ARTICLES
Published on Web 12/29/2007

Solid-State ^{19}F NMR Spectroscopy Reveals That Trp_{41} Participates in the Gating Mechanism of the M2 Proton Channel of Influenza A Virus

Raiker Witter,[†] Farhod Nozirov,[‡] Ulrich Sternberg,[†] Timothy A. Cross,[‡,§] Anne S. Ulrich,*[,||] and Riqiang Fu*[,‡]

Forschungszentrum Karlsruhe, IBG, POB 3640, 76021 Karlsruhe, Germany, National High Magnetic Field Laboratory, 1800 East Paul Dirac Drive, Tallahassee, Florida 32310, Department of Chemistry and Biochemistry, Institute of Biophysics, Florida State University, Tallahassee, Florida 32306, and Institut für Organische Chemie, University of Karlsruhe, Fritz-Haber-Weg 6, 76131 Karlsruhe, Germany

Received July 20, 2007; E-mail: rfu@magnet.fsu.edu; anne.ulrich@ibg.fzk.de

Abstract: The integral membrane protein M2 of influenza A virus assembles as a tetrameric bundle to form a proton-conducting channel that is activated by low pH. The side chain of His_{37} in the transmembrane α-helix is known to play an important role in the pH activation of the proton channel. It has also been suggested that Trp_{41}, which is located in an adjacent turn of the helix, forms part of the gating mechanism. Here, a synthetic 25-residue peptide containing the M2 transmembrane domain was labeled with 6F-Trp_{41} and studied in lipid membranes by solid-state ^{19}F NMR. We monitored the pH-dependent differences in the ^{19}F dipolar couplings and motionally narrowed chemical shift anisotropies of this 6F-Trp_{41} residue, and we discuss the pH activation mechanism of the H^+ channel. At pH 8.0, the structural parameters implicate an inactivated state, while at pH 5.3 the tryptophan conformation represents the activated state. With the aid of COSMOS force field simulations, we have obtained new side-chain torsion angles for Trp_{41} in the inactivated state ($\chi_1 = -100° \pm 10°$, $\chi_2 = +110° \pm 10°$), and we predict a most probable activated state with $\chi_1 = -50° \pm 10°$ and $\chi_2 = +115° \pm 10°$. We have also validated the torsion angles of His_{37} in the inactivated state as $\chi_1 = -175° \pm 10°$ and $\chi_2 = -170° \pm 10°$.

Introduction

A fundamental molecular and chemical aspect of ion channels concerns their mechanism of gating. The integral membrane protein M2 from influenza A virus forms a tetrameric bundle that acts as a pH-dependent proton-conductive channel[1−3] at two stages in viral replication. In a first stage, when the virus enters a cell and becomes embedded in an acidic compartment (pH 5−6), the M2 channel opens to import protons into the viron. The resulting change in protein−protein and protein−lipid interactions triggers the uncoating of the virus. Later on in the infection, M2 channels appear in the *trans*-Golgi network, where they balance the pH gradient across the membrane by exporting protons from the lumen to the cytoplasm. This proton-conductive channel has been characterized in considerable detail with regard to its structure−function relationship, such as its tetrameric state,[4−12] the backbone conformation of the trans-membrane (TM) domain,[13] and the role of the histidine tetrad in channel conductivity and proton selectivity.[3,14,15] However, the gating mechanism of the H^+ channel has not been fully understood, especially the role of the four tryptophans, which are located just one helical turn above the histidines. Here, we have characterized the tryptophan side-chain orientations of the TM domain of the M2 protein, incorporated in a lipid bilayer environment at different pH values, to understand its structural role in the opening and closing of the channel.

The M2 channel is a 97-residue protein with a 24-residue N-terminal and a 54-residue C-terminal segment connected by a single TM helix of 19 residues. Three hydrophilic residues, Ser_{31}, His_{37}, and Trp_{41}, are lining the pore, based on cysteine mutagenesis[16,17] and structural characterization of the TM

[†] Forschungszentrum Karlsruhe.
[‡] National High Magnetic Field Laboratory.
[§] Florida State University.
[||] University of Karlsruhe.

(1) Agmon, N. *Chem. Phys. Lett.* **1995**, *244*, 456−462.
(2) Pinto, L. H.; Holsinger, L. J.; Lamb, R. A. *Cell* **1992**, *69*, 517−528.
(3) Okada, A.; Miura, T.; Takeuchi, H. *Biochemistry* **2001**, *40*, 6053−6060.
(4) Sugrue, R. J.; Hay, A. J. *Virology* **1991**, *180*, 617−624.
(5) Sakaguchi, T.; Tu, O.; Pinto, L. H.; Lamb, R. A. *Proc. Natl. Acad. Sci. U.S.A.* **1997**, *94*, 5000−5005.
(6) Kochendoerfer, G. G.; Salom, D.; Lear, J. D.; Wilk-Orescan, R.; Kent, S. B.; DeGrado, W. F. *Biochemistry* **1999**, *38*, 11905−11913.
(7) Holsinger, L. J.; Nichani, D.; Pinto, L. H.; Lamb, R. A. *J. Virol.* **1994**, *68*, 1551−1563.
(8) Chizhmakov, I. V.; Geraghty, F. M.; Ogden, D. C.; Hayhurst, A.; Antoniou, M.; Hay, A. J. *J. Physiol.* **1996**, *494*, 329−336.
(9) Czabotar, P. E.; Martin, S. R.; Hay, A. J. *Virus Res.* **2004**, *99*, 57−61.
(10) Kelly, M. L.; James, J. A.; Brown-Augsburger, P.; Heinz, B. A.; Smith, M. C.; Pinto, L. H. *FEBS Lett.* **2003**, *552*, 61−67.
(11) Takeuchi, K.; Lamb, R. A. *J. Virol.* **1994**, *68*, 911−919.
(12) Lear, J. D. *FEBS Lett.* **2003**, *552*, 17−22.
(13) Nishimura, K.; Kim, S. G.; Zhang, L.; Cross, T. A. *Biochemistry* **2002**, *41*, 13170−13177.
(14) Hu, J.; Fu, R.; Nishimura, K.; Zhang, L.; Zhou, H. X.; Busath, D. D.; Vijayvergiya, V.; Cross, T. A. *Proc. Natl. Acad. Sci. U.S.A.* **2006**, *103*, 6865−6870.
(15) Wang, C.; Lamb, R. A.; Pinto, L. H. *Biophys. J.* **1995**, *69*, 1363−1371.

10.1021/ja0754305 CCC: $40.75

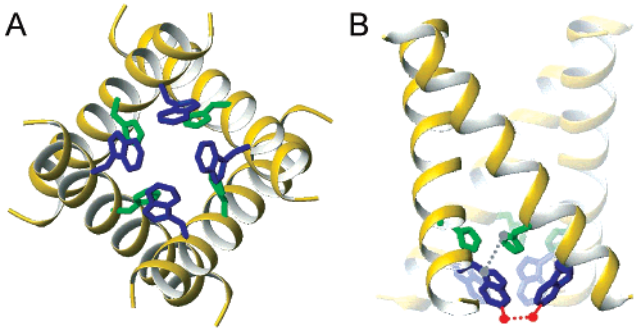

Figure 1. TM part of the M2 proton channel, illustrating the His_{37} (green) and Trp_{41} (blue) interactions in the four-helix bundle that control the gating mechanism. The conformations of the Nishimura model[13] at pH 8.0 are used, with His_{37} (χ_1, χ_2) = (−177°, +172°) and Trp_{41} (χ_1, χ_2) = (−177°, −105°). NMR distance constraints measured previously between His_{37} and Trp_{41} are indicated in gray, and shown in red are the new distances between 6F-Trp being addressed here. (A) Bottom view. (B) Side view.

domain.[13] The functional core of the channel is the TM α-helix assembled into a tetrameric channel structure.[7−9] The M2 channel conducts protons that are essential for viral replication.[1−3] The channel can be blocked by Cu^{2+},[8] amantadine,[18−20] and rimantadine,[21] specific anti-influenza A drugs that inhibit viral replication, primarily by binding to the M2 protein and thereby preventing proton conductance. Such binding influences chemically, dynamically, and structurally the TM domain of the M2 protein,[22,23] although the binding mechanism remains unclear. Unfortunately, these antiviral drugs have had limited clinical uses because of some severe side effects. Since 2005, the National Institute of Allergy and Infectious Diseases has no longer advised treatment with these drugs because of increasing viral resistance.[24] Therefore, understanding the structural basis for the opening and closing mechanism of the channel would allow us to understand the channel gating mechanism and thus provide a much needed guideline for designing new and more effective drugs that target this virus.

It has been shown that the acidification of the His_{37} side chains plays a crucial role in the activation of the M2 proton channel,[3,14,15] while the Trp_{41} residues are also functionally important. Mutagenesis investigations on Trp_{41} demonstrated a strong influence of the tryptophan side chains on proton conductance.[25] UV Raman data[3] provided evidence of a cation-π interaction between the protonated imidazole ring of His_{37} and the indole group of Trp_{41}, with a transition midpoint at pH 5.7. This investigation, however, showed that there is only a small pH-dependent conformational change of Trp_{41}, as its χ_2 torsion angle was found to remain close to 100°. A fluorescence study of the M2 protein demonstrated a pH dependence of the Trp_{41} and His_{37} interactions.[9] This evidence has supported the contention that the indole side chains form a steric block or gate for the proton conductance of the channel.

Here, we investigate a synthetic 25-residue (SSDPLVVAAS-$IIGILH_{37}LILW_{41}$ILDRL) peptide that forms the TM domain of the M2 protein (called M2TMD), containing the hydrophobic TM domain (P_{25}-L_{43}). The backbone structure of this peptide has been previously resolved, as shown in Figure 1, from solid-state NMR polarization inversion spin exchange at the magic angle (PISEMA) spectra of aligned samples,[13] in which the regular polarity index slant angle (PISA) wheel[26] demonstrates that residues 26−43 are entirely helical.[27] It has also been demonstrated that such an isolated TM domain of the M2 conducts protons.[14,28]

In this work, M2TMD was synthesized with 6-fluoro-tryptophan (6F-Trp), which is an ideal reporter group for highly sensitive solid-state ^{19}F NMR observation.[29−31] This ^{19}F chemical shift (CS) of 6F-Trp_{41} was measured at high and low pH values, corresponding to the pH-inactivated and -activated states of the channel. The structural interpretation can thus suggest whether this side chain participates in proton conductivity, and whether the four Trp_{41} residues interact with the imidazole rings of the hydrogen-bonded His_{37} network. On the basis of a correlation between the CS tensor elements and the $^{19}F-^{19}F$ dipolar coupling values, we thus restrain the structure of the gate in the activated and inactivated states.

Materials and Methods

Sample Preparation. 1,2-Dimyristoyl-*sn*-glycero-3-phosphocholine (DMPC) was purchased from Avanti Polar Lipids, Inc. and used as delivered. The synthesis of 6F-Trp_{41}-M2TMD was based on the solid-phase methods using an Applied Biosystems model 433A peptide synthesizer according to the literature.[32] The sample was purified according to Kovacs and Cross[32] and then codissolved with DMPC in methanol/chloroform[33] followed by evaporation of the organic solvents with a stream of N_2. The M2TMD/lipid film (20 mg/75 mg, i.e., molar ratio of 1:16) was dried under vacuum overnight and subsequently hydrated with 5 mM phosphate buffer with an adjusted pH (typically 1 mL). The vesicle suspension was incubated at 315 K for about 12 h and then concentrated using an ultracentrifuge (Beckman Coulter, Inc.) with 40000 rpm for 2 h. The pellets were kept for about 4 days in a dry silicate chamber to remove excess water. The pellets were finally rehydrated (to 60% by weight) and then transferred into 4-mm ZrO NMR rotors with Vespel sealing caps for NMR measurements. The sample was frozen and thawed several times from liquid nitrogen temperature.

NMR Spectroscopy. All ^{19}F NMR experiments were performed on a Bruker DRX600 NMR spectrometer, with ^{1}H and ^{19}F resonance frequencies of 600.1 and 564.1 MHz, respectively, using a Bruker triple resonance 4-mm H/F/X MAS NMR probe. Band selective filters

(16) Pinto, L. H.; Dieckmann, G. R.; Gandhi, C. S.; Papworth, C. G.; Braman, J.; Shaughnessy, M. A.; Lear, J. D.; Lamb, R. A. *Proc. Natl. Acad. Sci. U.S.A.* **1994**, *94*, 11301−11306.
(17) Bauer, C. M.; Pinto, L. H.; Cross, T. A.; Lamb, R. A. *Virology* **1999**, *254*, 196−209.
(18) Wang, C.; Takeuchi, K.; Pinto, L. H.; Lamb, R. A. *J. Virol.* **1993**, *67*, 5585−5594.
(19) Hay, A. J. *Semin. Virol.* **1992**, *3*, 21−30.
(20) Hay, A. J.; Wolstenholme, A. J.; Skehel, J. J.; Smith, M. H. *EMBO J.* **1985**, *4*, 3021−3024.
(21) Dolin, R.; Reichmann, R. C.; Madore, H. P.; Linton, P. N.; Webber-Jones, J. *N. Engl. J. Med.* **1982**, *307*, 580.
(22) Hu, J.; Asbury, T. M.; Achuthan, S.; Li, C.; Bertram, R.; Quine, J.; Fu, R.; Cross, T. A. *Biophys. J.* **2007**, *92*, 4335−4343.
(23) Hu, J.; Fu, R.; Cross, T. A. *Biophys. J.* **2007**, *93*, 276−283.
(24) Jefferson, T.; Demicheli, V.; Rivetti, D.; Jones, M.; Di Pietrantonj, C.; Rivetti, A. *Lancet* **2006**, *367*, 303−313.
(25) Tang, Y. J.; Zaitseva, F.; Lamb, R. A.; Pinto, L. H. *J. Biol. Chem.* **2002**, *277*, 39880−39886.
(26) Marassi, F. M.; Opella, S. J. *J. Magn. Reson.* **2000**, *144*, 150−155.
(27) Wang, J. F.; Kim, S.; Kovacs, F.; Cross, T. A. *Protein Sci.* **2001**, *10*, 2241−2250.
(28) Duff, K. C.; Ashley, R. H. *Virology* **1992**, *190*, 485−489.
(29) Ulrich, A. S. *Prog. Nucl. Magn. Reson. Spectrosc.* **2005**, *46*, 1−21.
(30) Ulrich, A. S.; Wadhwani, P.; Dürr, U. H. N.; Afonin, S.; Glaser, R. W.; Strandberg, E.; Tremouilhac, P.; Sachse, C.; Berditchevskaia, M.; Grage, S. In *NMR Spectroscopy of Biological Solids;* Ramamoorthy, A., Ed.; Taylor & Francis: Boca Raton, FL, 2006; pp 215−236.
(31) Grage, S. L.; Wang, J. F.; Cross, T. A.; Ulrich, A. S. *Biophys. J.* **2002**, *83*, 3336−3350.
(32) Kovacs, F. A.; Cross, T. A. *Biophys. J.* **1997**, *73*, 2511−2517.
(33) Chekmenev, E. Y.; Hu, J.; Gor'kov, P. L.; Brey, W. W.; Cross, T. A.; Ruuge, A.; Smirnov, A. I. *J. Magn. Reson.* **2005**, *173*, 322−327.

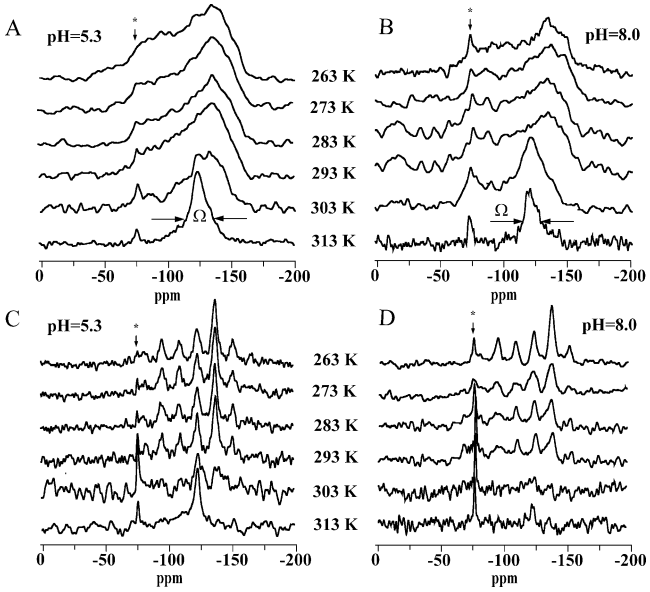

Figure 2. Static (A, B) and 8.0 kHz MAS (C, D) ^{19}F NMR spectra of 6F-Trp$_{41}$-M2TMD in DMPC (1:16 mol/mol) at pH = 5.3 (i.e., the pH-activated state: A, C) and pH = 8.0 (i.e., the pH-inactivated state: B, D). At 313 K, the rotationally averaged chemical shift spans were obtained: pH = 5.3 with 20 ppm < Ω < 30 ppm; and pH = 8.0 with 10 ppm < Ω < 20 ppm. The resonance from residual trifluoroethanol in the sample is indicated by an asterisk.

(Bruker) and band stop filters for both channels were used to provide sufficient isolation between the ^{1}H and ^{19}F channels. All spectra of the M2TMD peptide were obtained with 4 k scans and a repetition time of 5 s, using a standard spin−echo pulse sequence (90° pulse width of 3 μs) with proton decoupling (B_1 = 75 kHz). High-resolution ^{19}F NMR measurements were performed under static and magic-angle spinning (MAS) conditions at different temperatures. The spinning rates were controlled to within ±3 Hz, and the air temperature was controlled within ±0.1 K by a Bruker BVT-2000 unit. However, the sample temperature was expected to have a larger variation due to the sample heating during high power ^{1}H decoupling and/or MAS.[34−36] A 30 mM NaF solution was used as the external ^{19}F chemical shift reference (−120 ppm at 313 K).[37]

Force Field Simulations. For energy calculations, the COSMOS-NMR force field[38] was used with anharmonic potentials and an electrostatic energy utilizing coordinate-dependent atomic charges that were based on the semiempirical bond polarization theory (BPT). The BPT charges were parametrized on 6-31g(d,p) *ab initio* values from a natural population analysis.[39] The initial three-dimensional structure was obtained from the PDB (1NYJ).

Results

Figure 2 shows the static and MAS ^{19}F NMR spectra of the 6F-Trp$_{41}$-M2TMD peptide incorporated in hydrated DMPC at different pH values over a range of temperatures. At low pH = 5.3, the channel is in the pH-activated state, while at high pH = 8.0 the channel is in the pH-inactivated state. At temperatures below 273 K, the static ^{19}F spectra for both samples at pH 5.3 and 8.0 show a typical static powder line shape with a chemical shift span, Ω, of about 75 ppm. Above the lipid phase transition temperature (i.e., 313 K), the spectra are dramatically narrowed because of the rotation of the M2TMD channel around the channel axis in the liquid crystalline bilayers. The motionally averaged chemical shift span Ω is in a range of 10−20 ppm at pH 8.0, while it is 20−30 ppm at pH 5.3. This difference implies that the Trp side-chain orientations (with respect to the axis of averaging) differ in the pH-activated and -inactivated states of the channel. It is worth noting that at pH 8.0 the ^{19}F spectrum at 313 K has a very low signal-to-noise ratio compared to that at lower temperatures, despite the fact that the chemical shift anisotropy is narrowed by the rotation of the channel around the bilayer normal. This implies that the frequency scale of the dynamics (such as helical motion and/or the global wobble of the channel) in the inactivated state is different and less favorable for NMR observation. Figure 2C,D shows the ^{19}F MAS NMR spectra of the 6F-Trp$_{41}$-M2TMD peptide incorporated in hydrated DMPC at pH 5.3 and 8.0 at a spinning rate of 8.0 kHz. For both samples, the isotropic signal at −120 ppm appears to be independent of temperature. For pH 5.3, the pattern of the spinning sidebands remains almost the same until the temperature is above 293 K. For pH 8.0, the pattern of the spinning sidebands at 263 K is slightly different from that at pH 5.3, especially for the first spinning sideband at around −105 ppm. It is noticeable from Figure 2D that the sideband pattern for pH 8.0 is significantly affected by temperatures above 263 K. For both of the samples at 303 K, the spectral intensity becomes very weak, probably because the phase transition of the lipids introduces additional dynamics such as wobbling motions of the channel. Well above the lipid phase transition, at 313 K the isotropic peak gains intensity for pH 5.3, but not for pH 8.0, again implying that the dynamic frequency scale in the pH-inactivated state of the channel is unfavorable for NMR observation.

Figure 3A,B shows the MAS spectra of the two hydrated samples at 263 K spinning at 6.5 kHz. The lower spinning speed used here gives rise to noticeably different patterns of the spinning sidebands for pH 5.3 and 8.0. This is particularly evident in spectral intensity of the first spinning sideband at −108 ppm. To reveal the spectral differences between these two states, we used the SIMPSON[40] program to simulate the spectra, as illustrated in Figure 3. At low pH, two chemically identical ^{19}F nuclei (due to the fourfold symmetry of the channel) were considered in the simulations, and their relative tensor orientations were systematically varied. For convenience, the Euler angles of the first CS tensor were set to $\alpha_1 = \beta_1 = \gamma_1 = 0°$, while the relative Euler angles of the second CS tensor (α_2, β_2, γ_2) as well as the F−F dipolar coupling ω_d and its orientation β_d with respect to the first CS tensor were varied. As shown in Figure 3C, the root mean square (rms) minimum yields δ_{iso} = −120 ppm, δ_{aniso} = 49 ppm, and η = 0.6 for the chemical shift tensor. From the rms plot of Figure 3E, it can be seen that at pH 5.3 the dipolar coupling is less than −700 Hz, which means that the distance between any two ^{19}F labels is at least 5.3 Å. The slope is very steep up to −200 Hz, which corresponds to a distance of 8 Å. This simulation strongly suggests that the

(34) Doty, F. D.; Kulkarni, J.; Turner, C.; Entzminger, G.; Bielecki, A. *J. Magn. Reson.* **2006**, *182*, 239.
(35) Li, C.; Mo, Y.; Hu, J.; Chekmenev, E.; Tian, C.; Gao, F. P.; Fu, R.; Gor'kov, P.; Brey, W.; Cross, T. A. *J. Magn. Reson.* **2006**, *180*, 51−57.
(36) Gor'kov, P. L.; Chekmenev, E. Y.; Li, C.; Cotten, M.; Buffy, J. J.; Traaseth, N. J.; Veglia, G.; Brey, W. W. *J. Magn. Reson.* **2007**, *185*, 77−93.
(37) Glaser, R. W.; Ulrich, A. S. *J. Magn. Reson.* **2003**, *164*, 104−114.
(38) Sternberg, U.; Koch, F.-Th.; Losso, P. *COSMOS: Computer Simulation of Molecular Systems;* COSMOS GbR: Jena, Germany, 2006; www.cosmos-software.de.
(39) Witter, R. *Three Dimensional Structure Elucidation with the COSMOS-NMR Force Field;* dissertation.de: Berlin, 2004.
(40) Bak, M.; Rasmussen, J. T.; Nielsen, N. C. *J. Magn. Reson.* **2000**, *147*, 296−330.

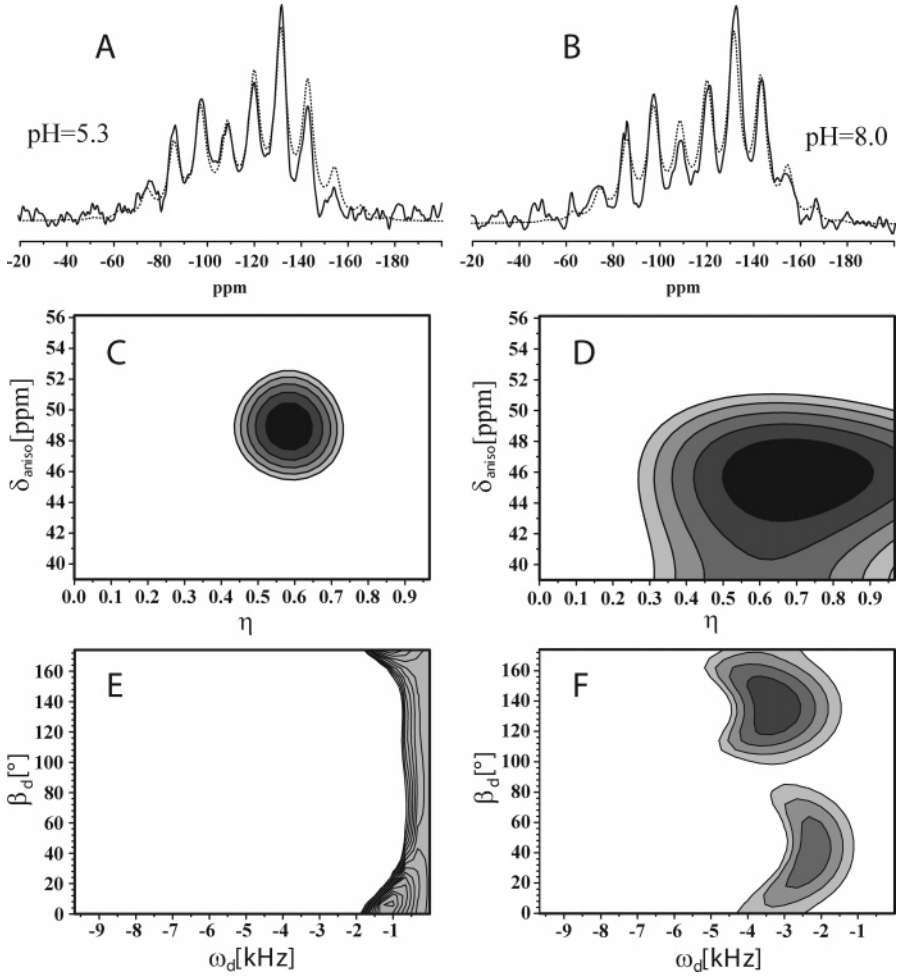

Figure 3. Experimental (solid lines) and simulated (dashed lines) spin−echo spectra of 6F-Trp$_{41}$-M2TMD at 6.5 kHz MAS at pH = 5.3 (A) and pH = 8.0 (B). For the SIMPSON spin−echo simulations, two chemically identical ^{19}F nuclei were assumed. (C and E) The pH-activated state of pH 5.3 the respective rms plots of the chemical shift anisotropy versus the asymmetry, and of the dipolar coupling angle β_d versus dipole frequency ω_d. (D and F) Corresponding rms plots for the pH-inactivated state at pH 8.0. Contour levels within 2% of minimum rms are shown from black to light gray.

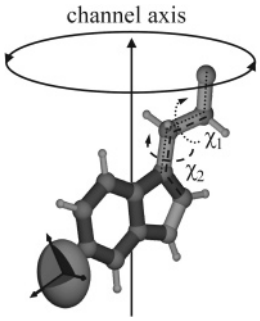

Figure 4. ^{19}F chemical shift tensor of a 6F-Trp fragment. For all further investigations, the following tensor components were used: $\delta_{11} = -71$ ppm (in C−F bond direction), $\delta_{22} = -130$ ppm (parallel to the indole π-plane), and $\delta_{33} = -159$ ppm (perpendicular to the indole π-plane). The rotational averaging along the channel axis along the bilayer is indicated. The side-chain torsion angles χ_1 and χ_2 are sketched.

indole rings of Trp$_{41}$ must be far apart from each other in the activated state of the tetrameric channel structure. From the PDB model (1NYJ),[13] the interhelical distance is about 8 Å, which was verified experimentally.[41] The F−F distance thus appears to be close to the value of 8 Å to produce such weak dipolar coupling. We consider this new structural information as a kind of anti-distance restraint.

Similarly, the spectrum in Figure 3B at high pH could be fitted, but only by introducing a larger F−F dipolar coupling in addition to the chemical shift tensors. We validated the experimentally obtained chemical shift parameters (Figure 3D: $\delta_{11} = -71$ ppm, $\delta_{22} = -130$ ppm, and $\delta_{33} = -159$ ppm) by *ab initio* Møller−Plesset perturbation theory (GIAO/MP2)[42,43] calculations with a tzvpp basis set[44−46] on a single Trp residue ($\delta_{11} = -64$ ppm, $\delta_{22} = -135$ ppm, and $\delta_{33} = -161$ ppm). We systematically varied the F−F dipolar coupling, ω_d, as well as the orientation of the dipolar axis with respect to the chemical shift tensor, β_d. From statistical error estimation (χ^2 of 16^2, and the partial derivative of the fitting function of 0.012/Hz gives an error of 1.3 kHz, as provided in the Supporting Information), the best fit yields a dipolar coupling frequency of $\omega_d = -3.1 \pm 1.3$ kHz, which corresponds to a F−F distance of 3.2 ± 0.3 Å. The two values of β_d in Figure 3F are found to be $\pm 40° \pm$

(41) Luo, W.; Hong, M. *J. Am. Chem. Soc.* **2006**, *128*, 7242−7251.
(42) Gauss, J. *Chem. Phys. Lett.* **1992**, *191*, 614−620.
(43) Gauss, J. *J. Chem. Phys.* **1993**, *99*, 3629−3643.
(44) Schafer, A.; Huber, C.; Ahlrichs, R. *J. Chem. Phys.* **1994**, *100*, 5829−5835.
(45) Weigend, F.; Haser, M.; Patzelt, H.; Ahlrichs, R. *Chem. Phys. Lett.* **1998**, *294*, 143−152.
(46) Ahlrichs, R.; Bar, M.; Haser, M.; Horn, H.; Kolmel, C. *Chem. Phys. Lett.* **1989**, *162*, 165−169.

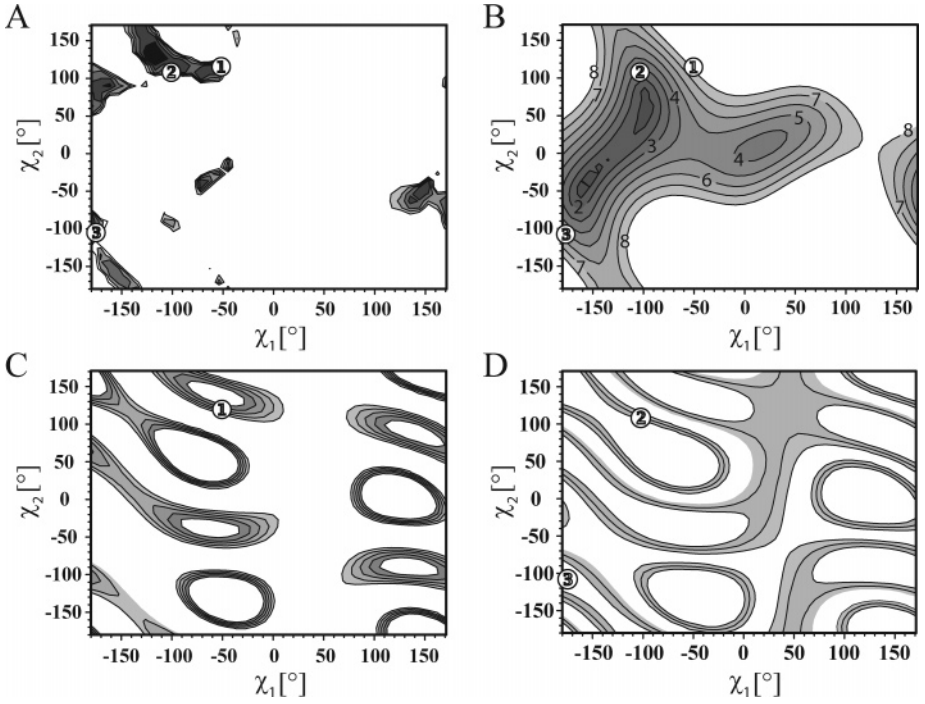

Figure 5. Maps of the total energy (A), the corresponding F−F distance (B), and the chemical shift spans at pH 5.3 (C) and pH 8.0 (D) as a function of the side-chain torsion angles χ_1 and χ_2 of 6F-Trp$_{41}$ in M2TMD embedded in DMPC. In the activated channel at pH 5.3, a unique combination of torsion angles that satisfy the anti-distance restraint and the allowed CS range of 20 ppm < Ω < 30 ppm is found at (χ_1, χ_2) = (−50° ± 10°, +115° ± 10°), as indicated by ① in (A)−(C). In the inactivated channel at pH 8.0, the distance constraint of 3.2 Å and the allowed CS range of 10 ppm < Ω < 20 ppm are consistent with (χ_1, χ_2) = (−100° ± 10°, +110° ± 10°) as indicated by ② in (A), (B), and (D). The opening of the channel thus corresponds to a transition from state ② to ①; the states are seen to be connected by a low-energy barrier, involving mainly a rotation around χ_1 by about 50°. For comparison, the previously suggested torsion angles (−177°, −105°) for the pH-inactivated state of the Nishimura model[13] are energetically supported, but incompatible with the experimental dipolar coupling and chemical shift, as illustrated by ③ in (A), (B) and (D).

15°. There are several possibilities for how to align the two CS tensors relative to another. For the fourfold symmetry, we consider the following rough tensor alignments: $\alpha_1 = \beta_1 = \gamma_1 = 0°$ and $\alpha_2 = 180°$, $\beta_2 = 90°$, $\gamma_2 = 0°$, and $\alpha_2 = 180°$, $\beta_2 = 90°$, $\gamma_2 = \pm 90°$.

Discussion

For the structural analysis of the M2 proton channel, we have now obtained an anti-distance constraint for the activated state at pH 5.3 (F−F distance of around 8 Å) under frozen conditions at 263 K. At high temperature (e.g., 313 K), the rotation of the channel about the membrane normal (i.e., the channel axis) scales the large ^{19}F chemical shift anisotropy significantly, as illustrated in Figure 4. Thus, the motionally averaged chemical shift span Ω carries the information about the Trp$_{41}$ side-chain orientation. At pH 5.3, the motionally averaged ^{19}F chemical shift span of 20 ppm < Ω < 30 ppm was measured at 313 K. For the inactivated state at pH 8.0, we determined a distance restraint of 3.2 Å and a residual chemical shift span of 10 ppm < Ω < 20 ppm. Furthermore, we can make use of the REDOR distance restraint from $^{15}N_\pi$−His$_{37}$−$^{13}C_\gamma$−Trp$_{41}$−M2TMD, which has been previously characterized from a dipolar coupling of 63 ± 12 Hz.[13] These distance restraints are illustrated in Figure 1B.

For the tetrameric peptide structure, there is a tight interaction between the histidines and tryptophans within the channel. Therefore, it cannot be considered a priori that a simple rotamer database will reflect the correct conformation of the Trp$_{41}$ side chain in M2TMD. Hence, we used COSMOS force field[38] total energy calculations without the aid of any constraint to map the total energy of the channel for all χ_1/χ_2 combinations of Trp$_{41}$. In contrast to other force fields, COSMOS includes anharmonic potentials and an electrostatic energy with coordinate-dependent atomic charges. The charge model is based on *ab initio* natural population analysis.[39] As an initial structure of M2TMD, the model from the PDB (1NYJ)[13] was used. The charged groups were modeled according to the respective pH values of the two samples. For the His$_{37}$ tetramer, we used the advanced protonation model according to the titration investigation by Hu et al.[14] At pH 5.3, the four His$_{37}$ side chains carry an averaged total charge of +3.1, while at pH 8.0 the total charge is around +1.3. Such a charged tetrameric M2TMD structure was placed into an equilibrated box with a size of 60^3 Å^3, containing 128 DMPC and 3000 water molecules. Under these conditions, all charges and energies, including the coordinate-dependent electrostatic interactions, were calculated for all possible conformations of the four Trp$_{41}$ residues on M2TMD. At this point of the investigation, the conformation of His$_{37}$ is unknown. To exclude any steric interactions between His$_{37}$ and Trp$_{41}$ side chains, His$_{37}$ was exchanged for glycine in the first round of simulations.

Figure 5A shows the calculated total energy as a function of the Trp$_{41}$ side-chain torsion angles χ_1 (N−C_α−C_β−C_γ) and χ_2 (C_α−C_β−C_γ−$C_{\delta 1}$). The minima in this map represent all allowed rotamers within the channel structure in a DMPC/water bilayer environment. Figure 5B shows the corresponding contour plot of the F−F distance calculated for the different χ_1/χ_2 combinations. Figure 5C,D shows the contour plots of the rotationally averaged chemical shift span Ω versus χ_1 and χ_2 in the two pH-controlled samples. The contour levels in Figure

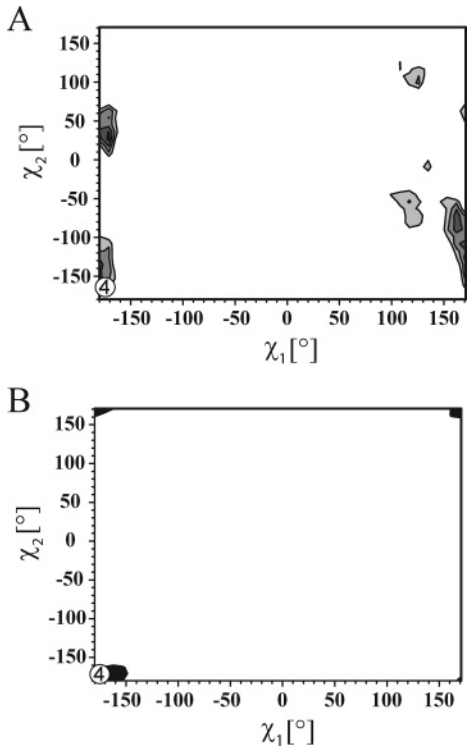

Figure 6. Maps of the total energy (A) and of the corresponding distance between $^{15}N_{\pi}-His_{37}$ and $^{13}C_{\gamma}-Trp_{41}$ (B), as a function of the side-chain torsion angles χ_1 and χ_2 of His_{37} in M2TMD in the inactivated state. The 63 ± 12 Hz range from dark to gray in steps of 5 Hz is shown. A unique solution is obtained as $(\chi_1, \chi_2) = (-175° \pm 10°, -170° \pm 10°)$, as indicated by ④, which is close to the Nishimura model (−177°, 172°).[13]

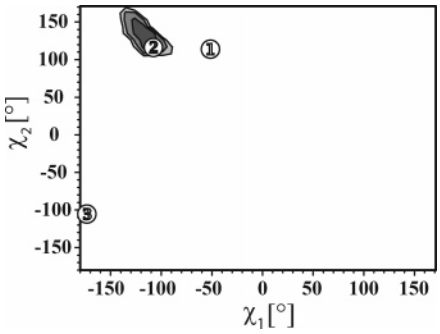

Figure 7. Map of the total energy as a function of the side-chain torsion angles χ_1 and χ_2 of 6F-Trp_{41} in M2TMD embedded in DMPC at pH 8.0 in the presence of His_{37} torsion angles (−175°, −170°).

5C were given for Ω ranging from 20 to 30 ppm in four steps, while the Ω values in Figure 5D were leveled from 10 to 20 ppm in three steps. Therefore, the strips between those contour levels in Figure 5C,D represent the experimentally allowed chemical shift spans. These maps show that there exists an energetically feasible side-chain conformation at pH 5.3 that is compatible with the allowed chemical shift span (Figure 5C) and with a long-range F−F distance of ∼8 Å (Figure 5B). These experimental restraints in combination with the total energy map (Figure 5A) thus yield a unique set of torsion angles of $(\chi_1, \chi_2) = (-50° \pm 10°, 115° \pm 10°)$ for the activated state, as indicated by ① in Figure 5. Likewise, for the inactivated state at pH 8.0, there appears to be a unique solution of $(\chi_1, \chi_2) = (-100° \pm 10°, 110° \pm 10°)$ that fulfils both the experimental restraints and the total energy map, as indicated by ②. Interestingly, it can be seen from Figure 5A that there is no high-energy barrier between the activated and inactivated states, and hence these conformations and their transition appear to be most probable.

For comparison with previous work, we also indicate by ③ the torsion angles $(\chi_1, \chi_2) = (-177°, -105°)$ obtained on the basis of a rotameric library by Nishimura et al.[13] Even though the latter torsion angles belong to an energetically allowed conformation, they do not fit our structural restraints, which might imply that the substitution of ^{19}F in the indole ring may have changed the side-chain orientation of Trp_{41}. However, in the labeling approach of Nishimura et al.,[13] the distance between $^{15}N_{\pi}-His_{37}$ and $^{13}C_{\gamma}-Trp_{41}$ is independent of χ_2. The only significant difference based on the experimental data is therefore in χ_1, namely −177° based on the N−C distance versus −100° based on our F−F distance.

By analogy with the Trp side-chain dipolar analysis, we used the total energy map together with the previously reported REDOR distance constraint[13] to validate the torsion angles of the His_{37} side chain in the presence of Trp_{41} with $(\chi_1, \chi_2) = (-100°, 110°)$ in the inactivated state. Figure 6 shows the calculated total energy and the contour plot of the residual dipolar coupling between $^{15}N_{\pi}-His_{37}$ and $^{13}C_{\gamma}-Trp_{41}$ as a function of the torsion angles of His_{37}, χ_1 ($N-C_{\alpha}-C_{\beta}-C_{\gamma}$) and χ_2 ($C_{\alpha}-C_{\beta}-C_{\gamma}-N_{\pi}$). Our data analysis yields a unique set of angles $(\chi_1, \chi_2) = (-175° \pm 10°, -170° \pm 10°)$, as indicated by ④, which is in good agreement with the previously reported His_{37} torsion angles (−177°, 172°) by Nishimura et al.[13]

To ensure the validity of the calculated total energy map in Figure 5A, the total energy as a function of the Trp_{41} side-chain torsion angles in the inactivated state was recalculated with our new His_{37} torsion angles (−175°, −170°). As shown in Figure 7, the total energy minimum appears at the torsion angles $(\chi_1, \chi_2) = (-100° \pm 10°, 120° \pm 10°)$, which is in good agreement with the initial calculation as indicated by ②, but not at the torsion angles marked by ① and ③ in Figure 5A. From this reiteration, it is evident that only the newly predicted angles $(\chi_1, \chi_2) = (-100° \pm 10°, 110° \pm 10°)$ are supported by all of the data in the inactivated state, while the Trp_{41} torsion angles indicated by ① are no longer allowed in the presence of the His_{37} torsion angles. This confirms that the steric effect of the His_{37} network strongly affects the Trp_{41} side-chain conformation.

From these ^{19}F NMR investigations, we have characterized for the first time the Trp_{41} side-chain conformation in the pH-activated state of the M2 proton channel, being $\chi_1 = -50° \pm 10°$ and $\chi_2 = 115° \pm 10°$ at pH 5.3. The corresponding molecular structure is illustrated in Figure 8A. For the pH-inactivated state at pH 8.0, we propose a new set of torsion angles for Trp_{41} ($\chi_1 = -100° \pm 10°$, $\chi_2 = 110° \pm 10°$), and we have confirmed the His_{37} conformation ($\chi_1 = -175° \pm 10°$, $\chi_2 = -170° \pm 10°$), as illustrated in Figure 8B. From this model, the average angle between ^{19}F CS tensor and dipole tensor is found to be $\beta_d \approx 40°$, which lies within 2% rms error of fitting results. It turns out that the Euler angles $\alpha_1 = \beta_1 = \gamma_1 = 0°$ and $\alpha_2 \approx 90°$, $\beta_2 \approx 90°$, $\gamma_2 \approx 0°$ are valid for the new closed conformation. The torsion angles obtained for Trp_{41} in M2TMD are also found for tryptophan in other proteins,[47] as for example $(\chi_1, \chi_2) = (-177°, -105°)$ for W126 in DsbA and W4 in NSCP;

(47) Hellings, M.; De Maeyer, M.; Verheyden, S.; Hao, Q.; Van Damme, E. J. M.; Peumans, W. J.; Engelborghs, Y. *Biophys. J.* **2003**, *85*, 1894−1902.

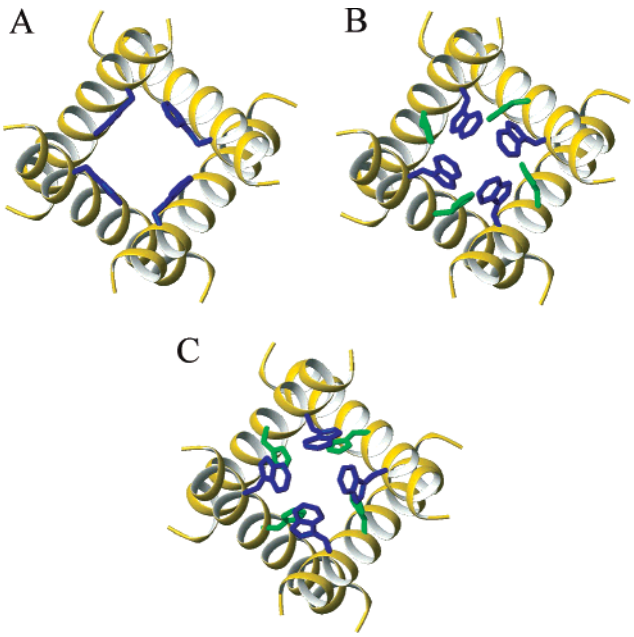

Figure 8. Side chain conformations (bottom view) of Trp_{41} (blue) and His_{37} (green) in the TM channel structure of the homotetrameric M2 protein. (A) The activated state at pH 5.3 for Trp_{41} (χ_1, χ_2) = (−50°, +115°). His_{37} torsion angles are not defined. (B) New coordinates for the inactivated state at pH 8.0 for His_{37} (−175°, −170°) and Trp_{41} (−100°, +110°). (C) Nishimura model[13] of the inactivated state for His_{37} (−177°, +172°) and Trp_{41} (−177°, −105°).

(−90°, +105°) for W175 in PAI-I and W140 in Colicin A; and (−50°, +115°) for W86 in Colicin A and W175 in PAI-I.

Our result is consistent with the previously published data on the histidine−tryptophan interaction. One model (UV Raman data)[3] had suggested only a small conformational change of Trp_{41} for the χ_2 torsion angle around 100°; indeed, we found no significant change (from 110° to 115°). Another model obtained by mutagenesis investigations,[25] which seemed to be contradictive to the UV Raman model, suggested strong conformational changes for tryptophan. Here, we were able to show that χ_1 is indeed responsible for a significant change from −100° to −50°.

In conclusion, through this solid-state ^{19}F NMR analysis in combination with computational energy calculations, we have demonstrated that the side-chain conformation and position of Trp_{41} differs significantly in the two pH-dependent states of the proton channel of M2TMD. The structural results in Figure 8 suggest that the four tryptophan residues actively participate in activating the channel mechanically. This response to a change in pH appears to be elicited via electrostatic and van der Waals interactions between His_{37} and Trp_{41}, which can thus be considered as a prerequisite for the gating mechanism. It appears that the role of the bulky Trp_{41} side chains is to enhance the steric effect of the His_{37} network that is directly involved in the H^+ gating. Due to the nature of large ^{19}F chemical shift anisotropy and the ability to access long-range F−F internuclear distances,[48] ^{19}F NMR is highly sensitive to subtle structural changes associated with the functional properties of ion channels as well as membrane proteins in general.[49−51] Thus, the kind of solid-state NMR analysis presented here is expected to become a most useful technique for characterizing structure−function dynamics relationships of membrane proteins in their "native" lipid environment.

Acknowledgment. This work was supported by the In-House Research Program at the National High Magnetic Field Laboratory (NHMFL). The NMR measurements were performed at NHMFL supported by the NSF Cooperative Agreement DMR-0084173 and the State of Florida. R.W., U.S., and A.S.U. thank the DFG-CFN Karlsruhe for financial support.

Supporting Information Available: Total energy calculations and spectral simulations. This material is available free of charge via the Internet at http://pubs.acs.org.

JA0754305

(48) Grage, S. L.; Suleymanova, A.; Afonin, S.; Wadhwani, P.; Ulrich, A. S. *J. Magn. Reson.* **2006**, *183*, 77−86.
(49) Strandberg, E.; Wadhwani, P.; Tremouilhac, P.; Dürr, U. H. N.; Ulrich, A. S. *Biophys. J.* **2006**, *90*, 1676−1686.
(50) Mikhailiuk, P. K.; Afonin, S.; Chernega, A. N.; Rusanov, E. B.; Platonov, M.; Dubinina, G.; Berditsch, M.; Ulrich, A. S.; Komarov, I. V. *Angew. Chem., Int. Ed.* **2006**, *45*, 5659−5661.
(51) Afonin, S.; Dürr, U. H. N.; Wadhwani, P.; Salgado, J. B.; Ulrich, A. S. In *Bioactive Conformation II;* Peters, T., Ed.; Topics in Current Chemistry 273; Springer: Berlin, 2008.